

Analytical Evaluation of Lead Iodide Precursor Impurities Affecting Halide Perovskite Device Performance

Ross A. Kerner,^a Earl D. Christensen,^a Steven P. Harvey,^a Jonah Messinger,^b Severin N. Habisreutinger,^a Fei Zhang,^{a,c} Giles E. Eperon,^d Laura T. Schelhas,^a Kai Zhu,^a Joseph J. Berry,^{a,e,f} and David T. Moore^a

a. National Renewable Energy Laboratory, Golden, Colorado 80401, USA

b. The Breakthrough Institute, Berkeley, California 94704, USA

c. School of Chemical Engineering and Technology, Tianjin University, Tianjin, 300072, China

d. Swift Solar Inc., 981 Bing St, San Carlos, California 94070, USA

e. Renewable and Sustainable Energy Institute, University of Colorado Boulder, Boulder Colorado 80309 USA

f. Department of Physics, University of Colorado Boulder, Boulder, Colorado 80309, USA

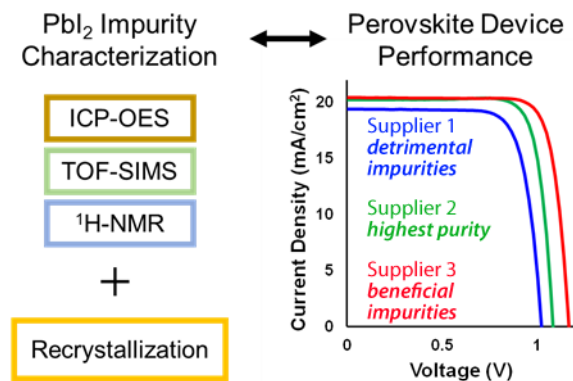
Corresponding Author

* David T. Moore: David.Moore@nrel.gov

Abstract

Mirroring established semiconductor technologies, halide perovskite materials synthesized from higher quality reagents display improved optoelectronic performance. In this study, we performed a semiquantitative analytical characterization of five different commercial PbI_2 sources to determine the identity and concentration of impurities that affect perovskite devices. It was possible to single out acetate (OAc) and potassium (K) as key species in as-received materials, both plausibly remnant from synthesis or purification. We removed these impurities through aqueous recrystallization revealing contrasting impacts on device performance: removal of OAc was beneficial but reducing K could be detrimental. This observation indicates that the highest purity PbI_2 does not guarantee the highest performing perovskite material, since certain extrinsic impurities, such as KI, can improve device performance. Fundamental and applied studies will both benefit from improved purification procedures coupled with analytical studies to better understand and control the effects of individual impurities in halide perovskite materials.

TOC GRAPHIC



Halide perovskite materials are touted as tolerant to the presence of native structural defects; native refers to “intrinsic” lattice point defects, including vacancies and interstitials, which may or may not be induced by an extrinsic impurity/defect.¹⁻³ That is to say, with the possible exception of positively charged iodine interstitials⁴, native defects are optoelectronically inert and do not prevent these materials from performing their primary photovoltaic or electroluminescent function.¹ This limited tolerance to crystallographic imperfections may mean native defects in perovskites are superficially benign, but their interactions with extrinsic species are certainly consequential. Reactions between native halide vacancies and molecular oxygen influence doping⁵ and facilitate degradation.^{6,7} Moreover, it is understood that concentrations of native defects and extrinsic impurities are directly linked. Ionic conductivity measurements of undoped and doped PbBr_2 crystals illustrate how, for example, Na^+ impurities occupying Pb^{2+} sites induce halide vacancies for charge neutrality, which are available to participate in ionic conduction.⁸ We speculate that halide perovskite defect populations are similarly dominated by impurities present within the reagents, a result of using processing additives, and released by *in situ* reactions during synthesis. Further, a growing body of literature⁹⁻¹⁸ indicates that the full efficiency and stability potential of halide perovskite materials will, to some degree, be unlocked by improving precursor quality, motivating us to scrutinize the impurity content of PbI_2 reagents for perovskite applications.

From this study, we present results from a semiquantitative analytical characterization of five commercially available PbI_2 materials. Three main techniques were used: inductively coupled plasma optical emission spectroscopy (ICP-OES) to determine I:Pb stoichiometry; ^1H and ^{13}C nuclear magnetic resonance (NMR) spectroscopy to reveal hydrogen-containing organic impurities; and time-of-flight secondary ion mass spectrometry (TOF-SIMS) to compare relative

intensities of lightweight atomic and molecular impurities. These techniques can be used separately or in combination to collect different information. For example, ICP-OES is ideal to quantify many elements, but molecular species such as organics, water, hydroxide, carbonate, or nitrate may need to be measured by other methods like NMR, ion chromatography, or titrations. A rigorous study on PbI_2 should evaluate purity along several axes for a comprehensive understanding of the impact of trace impurities on the resulting perovskite material quality and device performance.

Our analysis details two specific impurities in different source materials that were relatively abundant, positively identifiable, and successfully removed by aqueous recrystallization to measure an effect on devices. We found that iodide substoichiometry (I:Pb ratio < 2) was largely due to substitution of iodide by oxygen-containing anions including hydroxide (OH^-), proposed previously¹¹, as well as acetate (OAc) unambiguously identified in the lowest quality PbI_2 examined here. Oxidic impurities are notoriously difficult to remove from Pb halides,¹⁹ but reducing their concentration has been shown to have a positive effect on perovskite devices.¹¹ In contrast, the high quality PbI_2 sources investigated displayed relatively low concentrations of oxidic anion impurities. One PbI_2 reagent, in particular, simultaneously indicated elevated levels of potassium (K) and superstoichiometry (I:Pb > 2) suggesting KI as a plausible impurity. When oxidic anion concentrations are low, the beneficial effect of even small amounts of alkali iodide impurities like KI²⁰⁻²⁵ may become visible, helping to explain this PbI_2 's high material quality and device performance. Simply put, the beneficial effects of K can be easily overshadowed by other impurities. This was substantiated by purifying the as-received PbI_2 sources via aqueous recrystallization which reduced both OAc and adventitious K, among other impurities, and amended stoichiometries nearer to 2. Finally, we compared devices fabricated from all ten

as-received and recrystallized PbI_2 sources which, in combination with the analytical characterization, provides insight regarding dominant impurities and rationalizes expected outcomes in devices. Our work demonstrates that a competition can and does exist between beneficial (e.g. KI) and detrimental (e.g. oxidic anions) impurities which influence the overall performance of the materials at the device level.

While we suspect some impurities remain unidentified and/or unquantified, analytical verification of key species such as OAc and K allowed us to better explain observed differences in precursor solubility, deviation from nominal stoichiometry, and correlations to device performance. This work additionally demonstrates that common analytical techniques provide accessible means to evaluate purity levels of perovskite precursors and that practical purification methods can effectively raise the purity of most PbI_2 . These techniques are relevant to fundamental scientists for understanding the impact of synthetic conditions and intrinsic versus extrinsic material properties, as well as to applied scientists for tactics to improve quality control, performance, and reproducibility.

Abbreviations used throughout the manuscript for the five PbI_2 products, arranged according to measured stoichiometry, are shown in **Table 1**, along with their nominal purity, physical form, I:Pb ratio, and impurity information inferred from our data. The nomenclature is based on the supplier name and the number of “9s” in the quoted purity using metals basis or trace metals basis when reported.

Table 1. Abbreviation (Abbr.), product information, stoichiometry, solubility, and highlighted impurities suggested by SIMS and NMR data for the five commercial PbI₂ sources evaluated in this study, listed in order of I:Pb ratio measured by ICP-OES.

Abbr.	Supplier	Purity	Form	I:Pb ratio*	Solubility	Confirmed Impurities	Suspected Impurities
SA2	Sigma Aldrich	99%	Powder	1.84	Good	Na, K, OAc	OH ⁻ , O ²⁻
SA5	Sigma Aldrich	99.999%	Powder	1.92	Poor**	Na, K	OH ⁻ , O ²⁻ , OAc
AA4	Alfa Aesar	99.9985%	Powder	1.97	Poor	Na, K, organics	NO ₃ ⁻
TCI4	TCI	99.99%	Powder	2.03	Good		organics
AA5	Alfa Aesar	99.999%	Beads	2.10	Moderate	KI	

* ICP-OES data has an average error of +/- 5.8 % with a maximum error of +/- 6.7%

**Would not dissolve in perovskite inks precluding device fabrication.

Perfectly pure, stoichiometric PbI₂ should display an I:Pb ratio equal to two; therefore, stoichiometry is suggestive of overall purity or quality,¹⁵ but might not be predictively reliable. **Table 1** and **Fig. 1a** show I:Pb ratios of the as-received PbI₂ materials (measured by ICP-OES) varied from 8% deficient to 5% excess in iodide. Despite statistical considerations, the trend in as-received I:Pb ratio appears reflected in the corresponding device efficiency in **Fig. 1b** reported as stabilized power output (SPO). A similar trend in as-received PbI₂ efficiency is observed in devices with differing perovskite compositions, processing, and architectures made by different researchers (Supplementary Figures S1 and S2) confirming that the noted effects are not limited to a specific composition, architecture, nor processing route. Note that SA5 is omitted from as-received device sets because its solubility was too low to produce films adequate for devices.

We subsequently performed an aqueous recrystallization of all five PbI₂ sources to remove impurities that might alter the measured stoichiometry. As shown in **Fig. 1a**, the variation in I:Pb ratio was successfully reduced among the newly recrystallized (RC) PbI₂ reagents. Most

significant, the I:Pb ratio of the two outliers, SA2 and AA5, became statistically equivalent and much closer to two. Devices were fabricated from the recrystallized PbI_2 , and the measured SPO in **Fig. 1b** shows efficiency no longer correlates to the new stoichiometry. However, though it is significantly less obvious, the performance trend resembles that observed for the as-received materials. Note the recrystallized device data includes SA5 that became soluble after recrystallization, and the solubility of AA4 also improved slightly, which is a consistent improvement observed by several groups.^{11,13} This experiment illustrates that I:Pb ratio of the PbI_2 reagent has some influence on the perovskite quality, but it is not a reliable indicator of device efficiency. Device level metrics are likely dependent on the specific impurities that alter I:Pb ratio, so we turned to more in-depth characterization techniques to reveal the identity of the dominant impurity species.

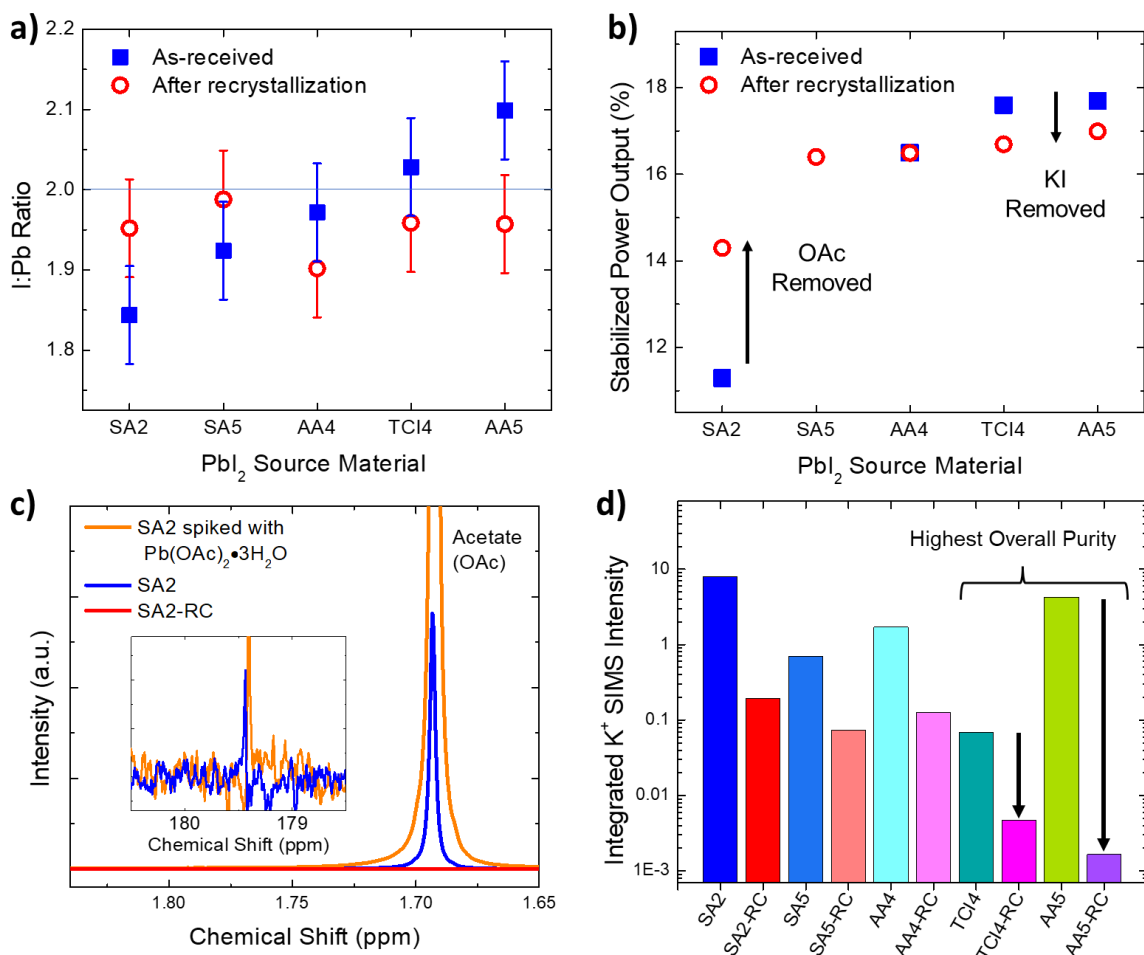


Figure 1. (a) I:Pb ratio measured by ICP-OES for as-received PbI_2 reagents compared to after aqueous recrystallization. (b) Stabilized power output (SPO) of devices fabricated with as-received and recrystallized PbI_2 precursors. (c) 1H -NMR of Sigma Aldrich 99% PbI_2 as-received (SA2), the SA2 sample spiked with a ~ 3 mg particle of lead acetate trihydrate ($Pb[OAc]_2 \cdot 3H_2O$), and a sample of recrystallized SA2 (SA2-RC). (d) Integrated SIMS K^+ ion intensity (summation of K counts normalized to total ion counts over 43 data points) of the PbI_2 powders as-received and after recrystallization (denoted by -RC suffix).

Using 1H -NMR, we identified OAc as a major anionic impurity in as-received SA2 (**Fig. 1c**) which we confirmed by spiking with lead acetate trihydrate and additional ^{13}C -NMR (inset).

Acetate is likely remnant from PbI_2 synthesis which commonly involves mixing water soluble $\text{Pb}(\text{OAc})_2$ or $\text{Pb}(\text{NO}_3)_2$ salts with KI to precipitate PbI_2 .^{12-14,26,27} Spiking experiments quantified the OAc concentration as $\sim 2.2 \pm 0.3$ mol% with respect to Pb (Supplementary Figure S3). It is particularly interesting to note the agreement between our inferred synthetic origin of SA2 and reports by Eckstein *et al.* that the $\text{Pb}(\text{OAc})_2$ route to PbI_2 typically results in lower stoichiometry than via $\text{Pb}(\text{NO}_3)_2$.²⁷ The measured amount of OAc accounts for only one fourth of the full 8% iodide deficiency in SA2, implying other extrinsic impurities are present in similar percentages. **Figure 1c** additionally shows that OAc was largely removed by the aqueous recrystallization to which we partially attribute the increase in stoichiometry and improved device performance for SA2 (**Fig. 1a** and **1b**). Since the OAc concentration, by itself, does not fully explain the device performance trends, either before or after recrystallization, we performed TOF-SIMS to identify species not detectable by NMR.

The most notable impurity we identified with TOF-SIMS was K, which also likely originates from synthesis. **Figure 1d** shows the integrated K^+ intensity of the PbI_2 materials as-received and after recrystallization (denoted by -RC suffix) highlighting large variation in relative K concentration by 3-4 orders of magnitude among the 10 different samples. The relative SIMS intensities for other alkali cations such as Li, Na, and Rb only varied by ~ 1 order of magnitude among the PbI_2 (Supplementary Figure S4), which justifies our focus on K in relation to changes in device performance. As-received, AA5 displays K^+ intensity 2 orders of magnitude higher than TCI4, the second-highest quality and most pure reagent (see below). Hydrocarbon/carbohydrate (**Fig. 2a**), oxide/hydroxide (**Fig. 2b**), and nitrogen oxide (**Fig. 2c**) SIMS fragment intensities suggest TCI4 and AA5 contain the lowest concentrations of oxygen-containing anion impurities (**Fig. 2a** fragment intensities further reflect significant OAc impurity in SA2²⁸). Together, these

two measurements on AA5 – low oxidic anion concentrations and I:Pb ratio greater than 2 – imply that KI is the main impurity in this commercial source. For all reagents except AA5, due to I:Pb \leq 2, the K impurities can be regarded as KOH, KOAc, or KNO₃. Potassium iodide is known as a beneficial processing additive for perovskite devices²⁰⁻²⁵, and residual KI in AA5 plausibly explains the observation that AA5-derived perovskites slightly outperform those processed from TCI4 in all our device data sets (**Fig. 1b** and Supplementary Fig. S1 and S2). Finally, recrystallization reduced K⁺ intensity in AA5 by nearly 3 orders of magnitude (**Fig. 1d**). The relative decrease in other alkali cations was a maximum of \sim 1 order of magnitude, again suggesting the large drop in K for AA5 is significant. Removing KI from a PbI₂ reagent free of anionic impurities is consistent with the observed decrease in ICP-OES stoichiometry (**Fig. 1a**) and lower device performance (**Fig. 1b**) after recrystallization.

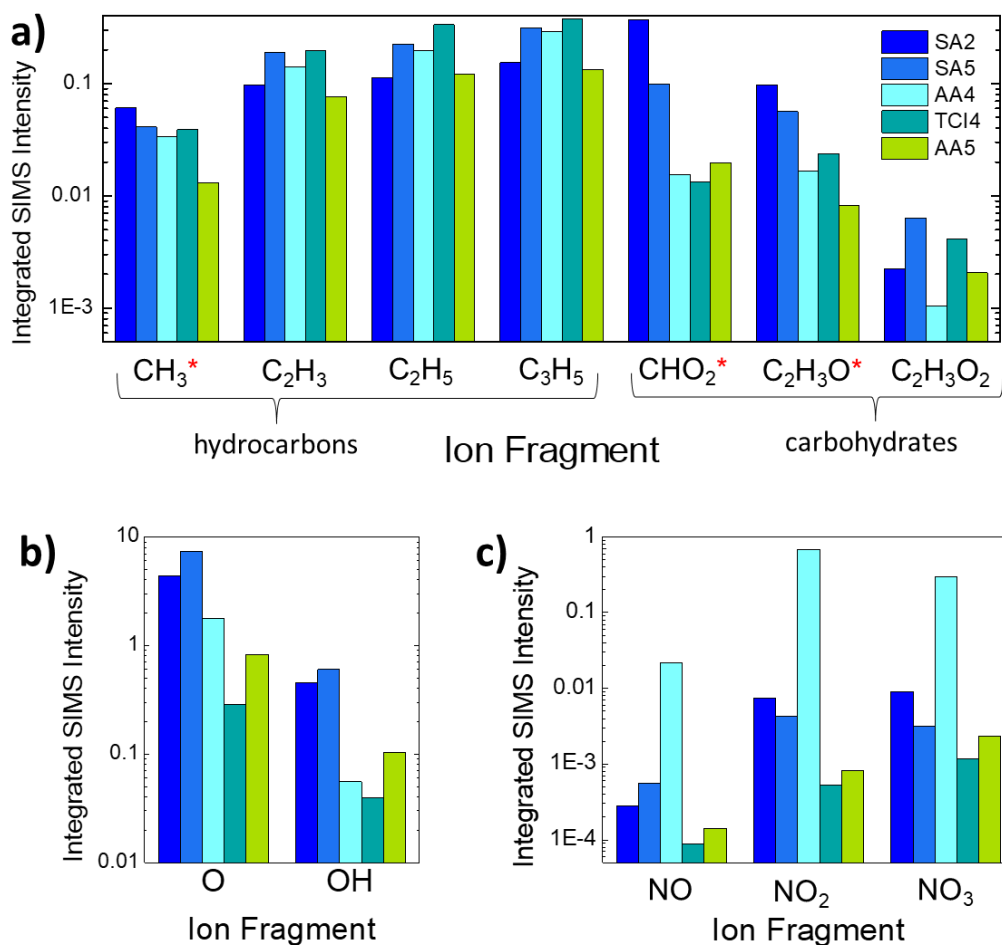


Figure 2. Integrated ion fragment SIMS intensities of (a) hydrocarbons and carbohydrates, (b) oxide and hydroxide, and (c) nitrogen oxides in the as-received PbI_2 sources. The fragments associated with acetate are indicated by * in (a).²⁸ Either TCI4 or AA5 displays the lowest intensity for each fragment.

The stoichiometry and device results are only partially explained by OAc and KI impurities, suggesting perovskite material quality is sensitive to other trace impurities that remain difficult to identify. For example, increased nitrogen oxide SIMS intensities for AA4 (**Fig. 2c**) suggest elevated nitrate impurities in this reagent that was removed by purification (Supplementary Figure S5). Indeed, several additional molecular impurities that might impact perovskite synthesis are

visible by $^1\text{H-NMR}$ of the as-received PbI_2s (**Fig. 3a**). There are unassigned, hydrogen-containing impurities present in all as-received PbI_2 sources except AA5 (SA2 additionally showed a small impurity peak downfield at 10.7 ppm). Recrystallized materials in **Fig. 3b** display reduced concentrations of original $^1\text{H-NMR}$ impurities (compare, for example, the quartet at 3.54 ppm in AA4 and AA4-RC in **Fig. 3a** and **Fig. 3b**, respectively), yet contain small signals from new impurities, one of which was identified as isopropanol (IPA, doublet at 0.99 ppm) that we used during filtration and collection. The NMR and additional SIMS data (Supplementary Fig. S4-S6) all indicate the recrystallization decreases impurity concentrations in most categories. However, OAc and K removal by recrystallization exemplify a competition between detrimental and beneficial impacts of impurities. Therefore, while recrystallizing PbI_2 may increase the purity, the degree to which the purified reagent improves the perovskite active layer and resulting devices may vary due to a given process's sensitivity to the trace beneficial impurities removed, as well as new trace species introduced, by the purification.

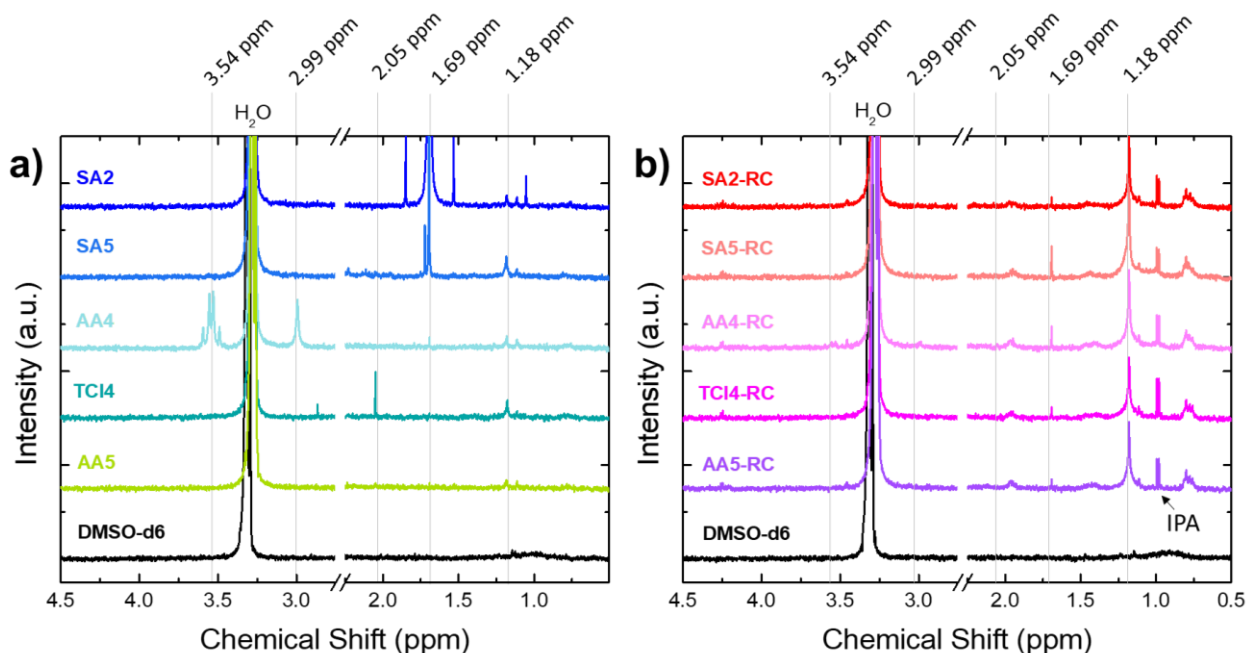


Figure 3. Upfield region ^1H -NMR spectra of PbI_2 sources as-received (a) and after aqueous recrystallization (b) denoted by -RC suffix (in deuterated dimethylsulfoxide [DMSO- d_6]). The DMSO- d_5 solvent peak is omitted by the x-axis break and several impurity peak positions are indicated for clarity.

Consequently, researchers may leverage this information about the different major impurities in as-received PbI_2 reagents or incorporate a purification protocol to best suit their goals. Our observations help rationalize difficulties reproducing results with PbI_2 from different suppliers or even batch-to-batch reproducibility from a single supplier. Improvements to purification methods and analytical characterization are necessary efforts for fundamental halide perovskite studies; accurate quantification of the impact of impurities and additives requires first reducing their levels to negligible concentrations before titrating back into the reagents. Ultimately, aqueous recrystallization methods may not achieve a desirable purity level nor optimal perovskite quality in devices, but alternative methods such as dissolution and precipitation from dimethylsulfoxide

(DMSO)¹¹ or sublimation in the dark (to avoid photolysis^{26,29,30}) under vacuum remain viable and should be simultaneously explored. Although the ideal purification technique relevant to perovskite semiconductors remains to be identified, fundamental- and device-oriented research will benefit from deeper analytical insight into perovskite precursors and the resulting materials.

In summary, we studied a set of five commercial PbI₂ precursor sources often used to fabricate halide perovskite devices. Cumulative information gathered from three analytical chemistry techniques elucidate relationships between synthesis, I:Pb stoichiometry, impurities, properties, and performance. We substantiated our conclusions by performing purifications via aqueous recrystallization and evaluated its effectiveness. Our semiquantitative analysis provides significant insight into specific impurities such as acetate and K that influence the functional performance of the resulting halide perovskite material. Identifying the remaining impurities, and optimizing purification methods, will help to clarify subtle yet impactful compositional variations that influence lab-to-lab or process-specific differences, and contribute to perovskites reaching their full potential. Like all semiconductor materials preceding it, the halide perovskite technology will undoubtedly benefit from rigorous scrutiny of precursor composition and purification methods.

ASSOCIATED CONTENT

Supporting Information. Detailed materials lists, device fabrication and testing, and characterization methods, performance results of two additional device composition-architectures using the commercial PbI₂ reagents, ¹H-NMR quantification of acetate figure, three figures with additional TOF-SIMS data.

AUTHOR INFORMATION

Corresponding author contact: David.Moore@nrel.gov

Notes

The authors declare no competing financial interest.

ACKNOWLEDGMENT

This work was authored by the National Renewable Energy Laboratory, operated by Alliance for Sustainable Energy, LLC, for the U.S. Department of Energy (DOE) under Contract No. DE-AC36-08GO28308. Funding provided by U.S. Department of Energy Office of Energy Efficiency and Renewable Energy, Solar Energy Technologies Office (SETO) project “De-risking Halide Perovskite Solar Cells” program (DE-FOA-0000990). R.A.K. acknowledges support from the Laboratory Directed Research and Development (LDRD) Program at NREL. The views expressed in the article do not necessarily represent the views of the DOE or the U.S. Government. The U.S. Government retains and the publisher, by accepting the article for publication, acknowledges that the U.S. Government retains a nonexclusive, paid-up, irrevocable, worldwide license to publish or reproduce the published form of this work, or allow others to do so, for U.S. Government purposes.

REFERENCES

1. Steirer, K. X.; Schulz, P.; Teeter, G.; Stevanovic, V.; Yang, M.; Zhu, K.; Berry, J. J. Defect Tolerance in Methylammonium Lead Triiodide Perovskite. *ACS Energy Lett.* **2016**, *1*, 360–366.

2. Walsh, A.; Scanlon, D. O.; Chen, S.; Gong, X. G.; Wei, S.-H. Self-Regulation Mechanism for Charged Point Defects in Hybrid Halide Perovskites. *Angew. Chem. Int. Ed.*, **2015**, *54*, 1791–1794.
3. Yin, W.-J.; Shi, T.; Yan, Y. Unusual defect physics in CH₃NH₃PbI₃ Perovskite Solar Cell Absorber. *Appl. Phys. Lett.*, **2014**, *104*, 063903.
4. Zhang, X.; Turiansky, M. E.; Shen, J.-X.; Van de Walle, C. G. Iodine Interstitials as a Cause of Nonradiative Recombination in Hybrid Perovskites. *Phys. Rev. B*, **2020**, *101*, 140101(R).
5. Shin, D.; Zu, F.; Cohen, A. V.; Yi, Y.; Kronik, L.; Koch, N. Mechanism and Timescales of Reversible p-Doping of Methylammonium Lead Triiodide by Oxygen. *Adv. Mater.*, **2021**, *33*, 2100211.
6. Aristidou, N.; Eames, C.; Sanchez-Molina, I.; Bu, X.; Kosco, J.; Islam, M. S.; Haque, S. A. Fast Oxygen Diffusion and Iodide Defects Mediate Oxygen-Induced Degradation of Perovskite Solar Cells. *Nat. Comm.*, **2017**, *8*, 15218.
7. Bryant, D.; Aristidou, N.; Pont, S.; Sanchez-Molina, I.; T. Chotchuangchutchaval, T.; Wheeler, S.; Durrant, J. R.; Haque, S. A. Light and Oxygen Induced Degradation Limits the Operational Stability of Methylammonium Lead Triiodide Perovskite Solar Cells. *Energy Environ. Sci.*, **2016**, *9*, 1655–1660.
8. Schoonman, J. The Ionic Conductivity of Pure and Doped Lead Bromide Single Crystals. *J. Solid State Chem.*, **1972**, *4*, 466–474.

9. Yao, J.; Yang, L.; Cai, F.; Yan, Y.; Gurney, R. S.; Liu, D.; Wang, T. The Impacts of PbI₂ Purity on the Morphology and Device Performance of One-step Spray-coated Planar Heterojunction Perovskite Solar Cells. *Sustain. Energy Fuels*, **2018**, *2*, 436–443.
10. Chang, J.; Zhu, H.; Li, B.; Isikgor, F. H.; Hao, Y.; Xu, Q.; Ouyang, J. Boosting the Performance of Planar Heterojunction Perovskite Solar Cell by Controlling the Precursor Purity of Perovskite Materials. *J. Mater. Chem. A*, **2016**, *4*, 887–893.
11. Senevirathna, D. C.; Yu, J. C.; Peiris, T. A. N.; Li, B.; Michalska, M.; Li, H.; Jasieniak, J. J. Impact of Anion Impurities in Commercial PbI₂ on Lead Halide Perovskite Films and Solar Cells. *ACS Materials Lett.* **2021**, *3*, 351–355.
12. Chen, B.; Fei, C.; Chen, S.; Gu, H.; Xiao, X.; Huang, J. Recycling Lead and Transparent Conductors from Perovskite Solar Modules. *Nat. Comm.* **2021**, *12*, 5859.
13. Lee, C.-H.; Shin, Y.-J.; Jeon, G. G.; Kang, D.; Jung, J.; Jeon, B.; Park, J.; Kim, J.; Yoon, S. J. Cost-efficient, Effect of Low-Quality PbI₂ Purification to Enhance Performances of Perovskite Quantum Dots and Perovskite Solar Cells. *Energies*, **2021**, *14*, 201.
14. Lee, C.-H.; Shin, Y.-J.; Villanueva-Antolí, A.; Adhikari, S. D.; Rodriguez-Pereira, J.; Macak, J. M.; Mesa, C. A.; Giménez, S.; Yoon, S. J.; Gualdrón-Reyes, A. F.; Mora-Seró, I. Efficient and Stable Blue- and Red-Emitting Perovskite Nanocrystals through Defect Engineering: PbX₂ Purification. *Chem. Mater.* **2021**, *33*, 8745–8757.
15. Tsevas, K.; Smith, J. A.; Kumar, V.; Rodenburg, C.; Fakis, M.; Yusoff, A. R. b. M.; Vasilopoulou, M.; Lidzey, D. G.; Nazeeruddin, M. K.; Dunbar, A. D. F. Controlling PbI₂

Stoichiometry during Synthesis to Improve the Performance of Perovskite Photovoltaics. *Chem. Mater.* **2021**, *33*, 554–566.

16. Min, H.; Kim, M.; Lee, S.-U.; Kim, H.; Choi, K.; Lee, J. H.; Seok, S. I. Efficient, Stable Solar Cells by Using Inherent Bandgap of α -phase Formamidinium Lead Iodide. *Science*, **2019**, *366*, 749–753.
17. Zhang, Y.; Seo, S.; Lim, S. Y.; Kim, Y.; Kim, S.-G.; Lee, D.-K.; Lee, S.-H.; Shin, H.; Cheong, H.; Park, N.-G. Achieving Reproducible and High-Efficiency (>21%) Perovskite Solar Cells with a Presynthesized FAPbI₃ Powder. *ACS Energy Lett.* **2020**, *5*, 360–366.
18. Tong, G.; Son, D.-Y.; Ono, L. K.; Kang, H.-B.; He, S.; Qiu, L.; Zhang, H.; Liu, Y.; Hieulle, J.; Qi, Y. Removal of Residual Compositions by Powder Engineering for High Efficiency Formamidinium-based Perovskite Solar Cells with Operation Lifetime Over 2000 h. *Nano Energy*, **2021**, *87*, 106152.
19. Tonna, J.; Matuchovab, M.; Danilewsky, A. N.; Cröll, A. Removal of Oxidic Impurities for the Growth of High Purity Lead Iodide Single Crystals. *J. Cryst. Growth*, **2015**, *416*, 82–89.
20. Zhao, W.; Yao, Z.; Yu, F.; Yang, D.; Liu, S. (F.). Alkali Metal Doping for Improved CH₃NH₃PbI₃ Perovskite Solar Cells. *Adv. Sci.*, **2018**, *5*, 1700131.
21. Tang, Z.; Bessho, T.; Awai, F.; Kinoshita, T.; Maitani, M. M.; Jono, R.; Murakami, T. N.; Wang, H.; Kubo, T.; Uchida, S.; Segawa, H. Hysteresis-free Perovskite Solar Cells Made of Potassium-doped Organometal Halide Perovskite. *Sci. Rep.*, **2017**, *7*, 12183.

22. Abdi-Jalebi, M.; Andaji-Garmaroudi, Z.; Cacovich, S.; Stavrakas, C.; Philippe, B.; Richter, J. M.; Alsari, M.; Booker, E. P.; Hutter, E. M.; Pearson, A. J.; Lilliu, S.; Savenije, T. J.; Rensmo, H.; Divitini, G.; Ducati, C.; Friend, R. H.; Stranks, S. D. Maximizing and stabilizing luminescence from halide perovskites with potassium passivation. *Nature*, **2018**, *555*, 497–501.
23. Yang, Y.; Wu, L.; Hao, X.; Tang, Z.; Lai, H.; Zhang, J.; Wang, W.; Feng, L. Beneficial effects of potassium iodide incorporation on grain boundaries and interfaces of perovskite solar cells. *RSC Adv.*, **2019**, *9*, 28561–28568.
24. Son, D.-Y.; Kim, S.-G.; Seo, J.-Y.; Lee, S.-H.; Hyun Jung Shin, H.; Lee, D.; Park, N.-G. Universal Approach toward Hysteresis-Free Perovskite Solar Cell via Defect Engineering. *J. Am. Chem. Soc.*, **2018**, *140*, 1358–1364.
25. Su, R.; Xu, Z.; Wu, J.; Luo, D.; Hu, Q.; Yang, W.; Yang, X.; Zhang, R.; Yu, H.; Russell, T. P.; Gong, Q.; Zhang, W.; Zhu, R. Dielectric screening in perovskite photovoltaics. *Nat. Comm.* **2021**, *12*, 2479.
26. Albrecht, M.G. (1975). The photolysis of lead iodide. PhD Thesis (University of London, Imperial College).
27. Eckstein, J.; Erler, B.; Benz, K. W. High purity lead iodide for crystal growth and its characterization. *Mater. Res. Bull.*, **1992**, *27*, 537–544.
28. NIST Standard Reference Database 69: NIST Chemistry WebBook Acetic acid (nist.gov), <https://webbook.nist.gov/cgi/cbook.cgi?ID=C64197&Units=SI&Mask=200#Mass-Spec>, date accessed 11/26/2021

29. Saucedo, E.; Fornaro, L.; Mussio, L.; Gancharov, A. New Ways for Purifying Lead Iodide Appropriate as Spectrometric Grade Material. *IEEE Trans. Nucl. Sci.*, **2002**, *49*, 1974–1977.
30. Fornaro, L.; Saucedo, E.; Mussio, L.; Yerman, L.; X. Ma, X.; Burger, A. Lead iodide film deposition and characterization. *Nucl. Instrum. Methods.*, **2001**, *458*, 406–412.